Design of compact UWB monopole patch antenna with octagonal shape for C-band, Wi-MAX, and WLAN applications

F. ABAYAJE[1], A. A. ALRAWACHY[1], Y. S. MEZAAL[2,3,*]
[1]*Department of Software, College of Computer Science and Mathematics, University of Mosul, Iraq*
[2]*Department of Mobile Communications and Computing Engineering, University of Information Technology and Communications, Baghdad, Iraq*
[3]*Visiting Researcher, Al-Farahidi University, Baghdad, Iraq*

This study presents a new compact UWB monopole antenna designed for 4G and 5G wireless band communications. The antenna features a partial ground plane and an octagonal radiation patch, which enable two resonances at 2.6 and 5 GHz bands with a bandwidth of S11 < -10 dB ranging from 2 – 6 GHz (4000 MHz). The antenna covers the frequencies of 3.7-4.2 GHz (C-band), 3.2-3.8 GHz (WiMAX band), and 5.15-5.85 GHz (WLAN band), making it suitable for various applications including wireless medical applications. Fabricated on an FR4 substrate with a dielectric constant of εr =4.4, loss tangent (tan δ)= 0.015, and thickness of 1.6 mm, the proposed antenna exhibits bi-directional and omnidirectional radiation patterns in the E and H-planes. Additionally, it offers advantages in terms of wireless baseband transmission at high data rates and in the near-field region. Compared to other UWB antennas in the literature, the presented antenna has very compact size of only 30 × 20 × 1.6 mm^3, making it easily integrable into various wireless medical terminals. The experimental results demonstrate the effectiveness and performance of the proposed antenna design.

(Received August 14, 2022; accepted August 7, 2023)

Keywords: Monopole antenna, FR4 material, WiMAX, WLAN, C-band, UWB antenna, Microstrip patch antenna

1. Introduction

As a result of its small size, high data resolution, and low spectral power density, the microstrip patch antenna has become a popular choice for modern wireless communication systems [1-3]. The demand for high-speed transmission from wireless communication systems is becoming more urgent, and various solutions have been proposed. To meet this requirement, attention has focused on wide-bandwidth antennas, as they offer many advantages, such as higher data rates, communication capability, operational security, less complexity, and less interference [4-6]. Bi-directional and Omni-directional radiation characteristics and a good gain response are desired to be well suited for narrow bands communication systems such as WLAN in ISM bands (2.4–2.5 GHz), Wi-MAX (3.4–3.7 GHz), high data rate WLAN IEEE 802.11a/h/j/n (5.15–5.825GHz) [7-11]. Ultra-wideband (UWB) antennas with dual-notched bands are reported in the literature using square rings [12] and microstrip patch with dual H-shaped slots [13]. On the other hand, UWB antennas without notched bands are reported in [14-19] using Antipodal Vivaldi, double-layer electronic bandgap (EBG) structures, and inductively-loaded dipole.

This research proposes UWB octagonal patch microstrip antenna with characteristics spanning 2 GHz to 6 GHz. It is possible to achieve resonance at 2.6 and 5 GHz by simply placing C-shaped slots in the ground plane. To simulate the design structure, HFSS 15.0 was used on FR4 substrate with dielectric constant (4.4), thickness (1.6 mm), and loss tangent of (0.015). The main goal of this article is to build an improved antenna for Wireless Baseband Transmission (WBT) and MIMO with better bandwidth than many existing antennas. In this paper, there is an explanation of the monopole antenna's geometry in Section 2. Section 3 discusses various findings of the simulation, while section 4 depicts the experimental result. Finally, section 5 shows the sweeping conclusions of this paper.

2. Design

Fig. 1 depicts the proposed broadband monopole antenna's geometry. The total monopole antenna surface area has been 30 × 20 mm^2. A feed-line microstrip width has been fixed at 3.44 mm for an impedance of 50-Ω from 2 GHz to 6 GHz bandwidth, satisfying the WLAN, WiMAX, and C-bands. In addition, for a good adaptation of the bandwidth, the radius of the circular and the small rectangle on the ground plane, which are printed on the back of the substrate, are indicated by *R* and *g* (see Fig. 1), which allows reasonable control of the lower and higher-frequency values for the antenna bandwidth.

3. Results and discussion

Fig. 2 illustrates the simulated input reflection of the design monopole antenna. As illustrated in the figure, the S11 parameter has been tuned to remain below -10 dB across the 2 to 6 GHz frequency band, with two resonant frequencies at 2.6 and 5 GHz.

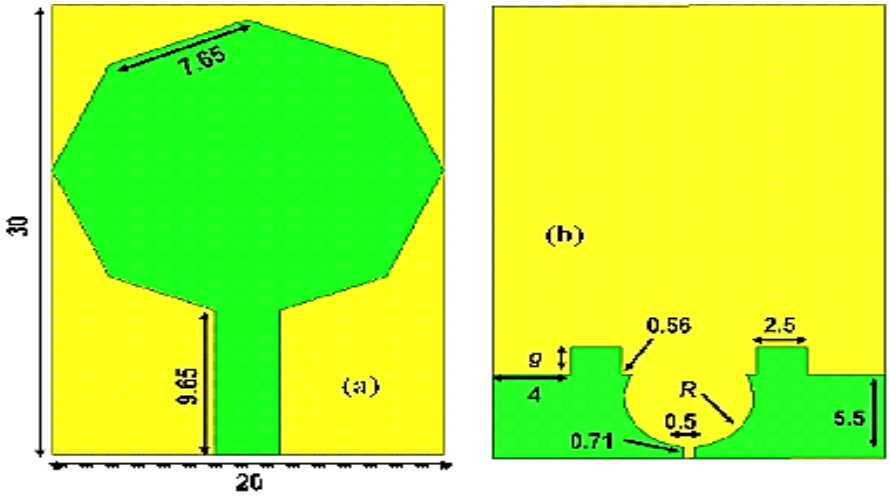

Fig. 1. Structure of the projected antenna with octagonal radiation patch and partial ground plane. Dimensions and parameters for the projected antenna (units: mm). g = 2.2 mm. R= 3.3 mm that is the radius of circular on the ground plane (color online)

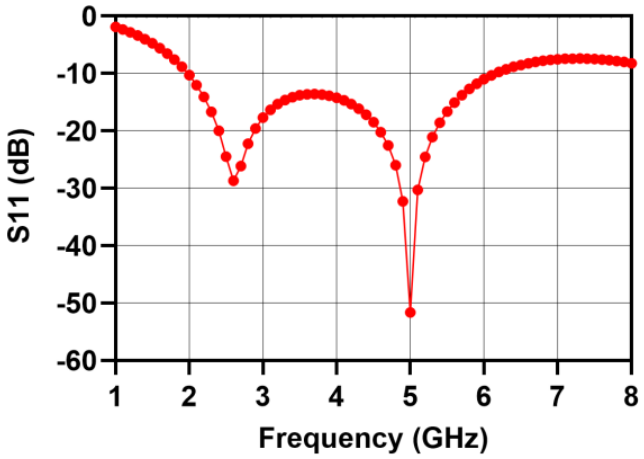

Fig. 2. Input reflection against the frequency of the antenna at f_r = 2.6, 5 GHz

Fig. 3 shows the effects of changing circular radius values on impedance matching in the band range. It can be seen in Fig. 3 that the resonant frequencies are shifted backward as the radius value increases. The input reflection varies between -24 to -52 dB with respect to circular radius values. The impedance bandwidth increases as the circular radius decreases. The value of the radius at R = 3.3 mm is considered in our design to obtain the needed UWB range of antenna, as shown in Fig. 2.

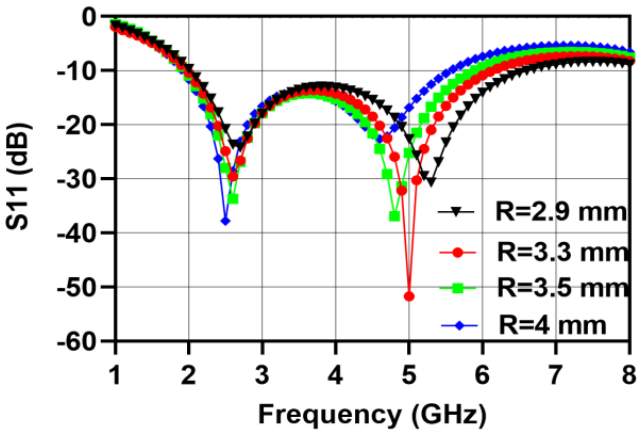

Fig. 3. Simulated variation of input reflection with frequency for the antenna with changed circular radius values (R) (color online)

Fig. 4 illustrates the values of variation of input reflection by changing the length of the small rectangle (g as in Fig. 1) for values of 1.7, 2.2, 2.5, and 2.6 mm with R= 3.3 mm. As shown in the figure, the simulated resonant frequency is shifted with the slight change in length of the rectangle, especially in the second resonant frequency (upper frequency) around 5 GHz. In contrast, the first (lower frequency) resonant frequency does not change. It is observable from the figure that the value g can miniaturize the bandwidth of the antenna by lowering the maximum working frequency, where g = 2.2 mm is considered in this design.

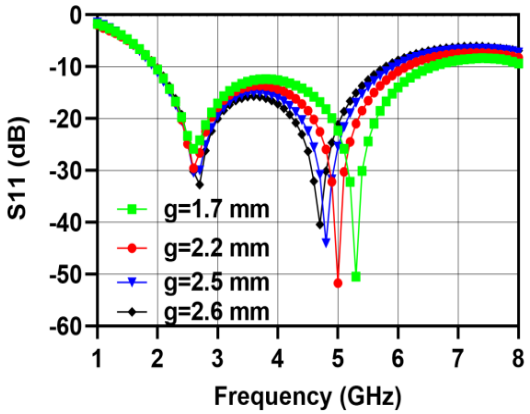

Fig. 4. Simulated variation of return loss with frequency for the antenna with R= 3.3 mm and the change of length values g (color online)

Fig. 5 illustrates the gain variation for the monopole antenna as a frequency function. In the frequency range of 1 to 8 GHz, the flat gain rises linearly with frequency over the entire operating band. The maximum gain is 2.62 dB at 8 GHz, which can enhance low-end performance. The gain bandwidth (3-dB) is less than the impedance bandwidth.

It is tolerable since the projected antenna is very compact and based on lossy substrate like FR4 material.

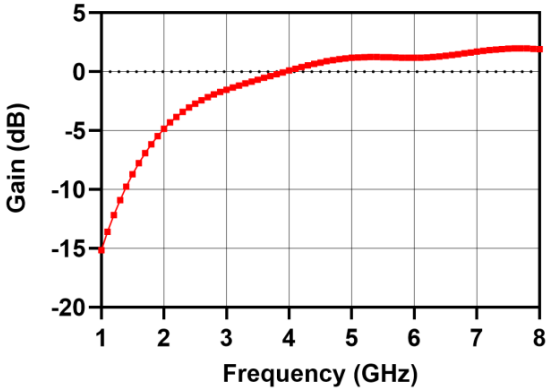

Fig. 5. Simulated variation of antenna gains with respect to frequency

Co-polarization and cross-polarization at 2.6, 5, and 7 GHz in E-plane and H-plane are depicted in Fig. 6. As presented in this figure, the radiation pattern for the monopole antenna exhibits bi-directional and omnidirectional far-field patterns.

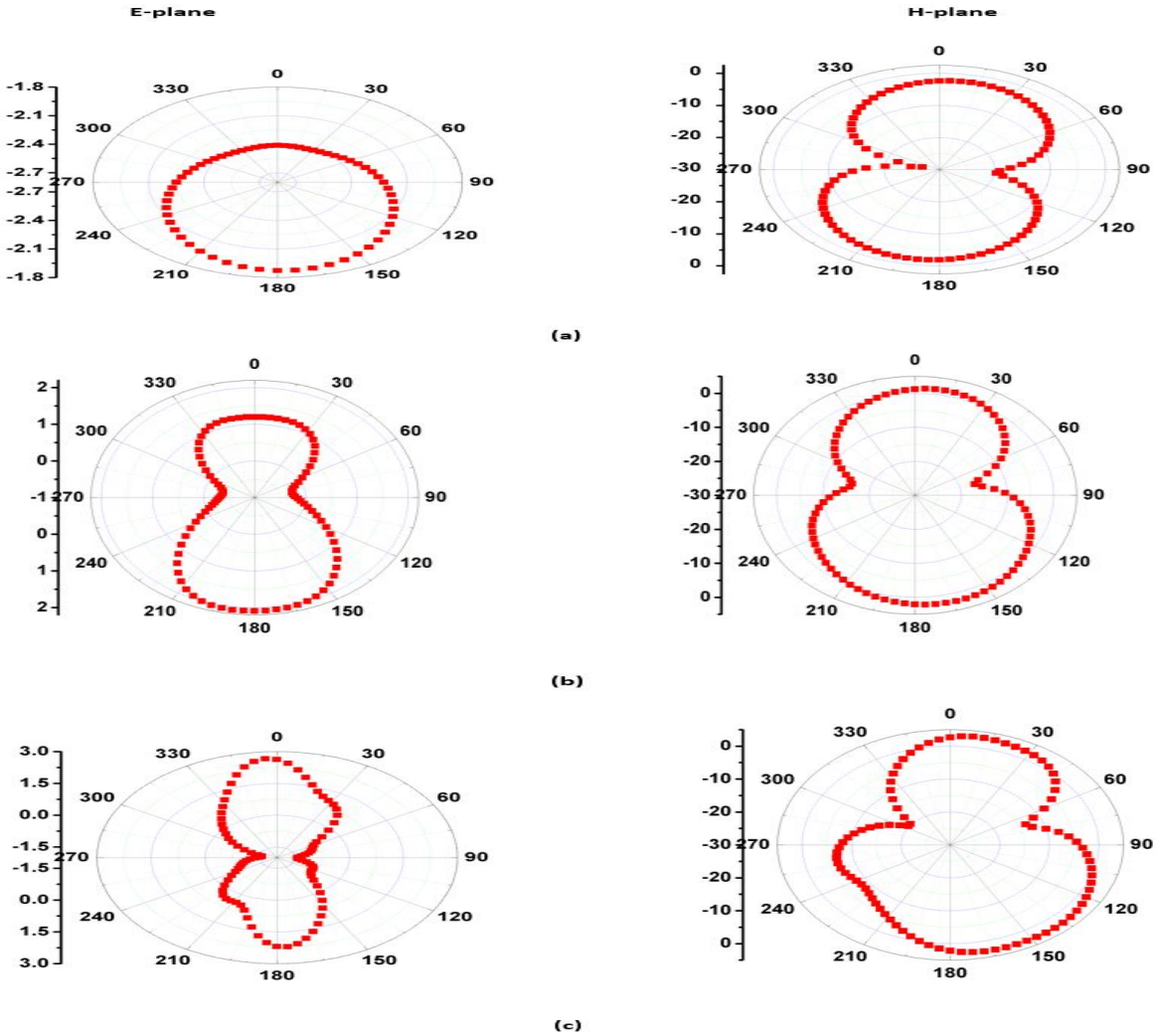

Fig. 6. E-plane (x-z) and H-plane (y-z) radiation pattern of the antenna at (a) 2.6, (b) 5, and (c) 7 GHz

Figs. 7 and 8 depict the effective surface current distributions for monopole patch and ground planes at 2.6 and 5 GHz. The effective regions are in octagonal patch boundaries and ground plane boundaries at the lower resonant frequency. On the other hand, at the upper resonance, the effective areas are also in octagonal patch and ground plane boundaries but with stronger electric intensities.

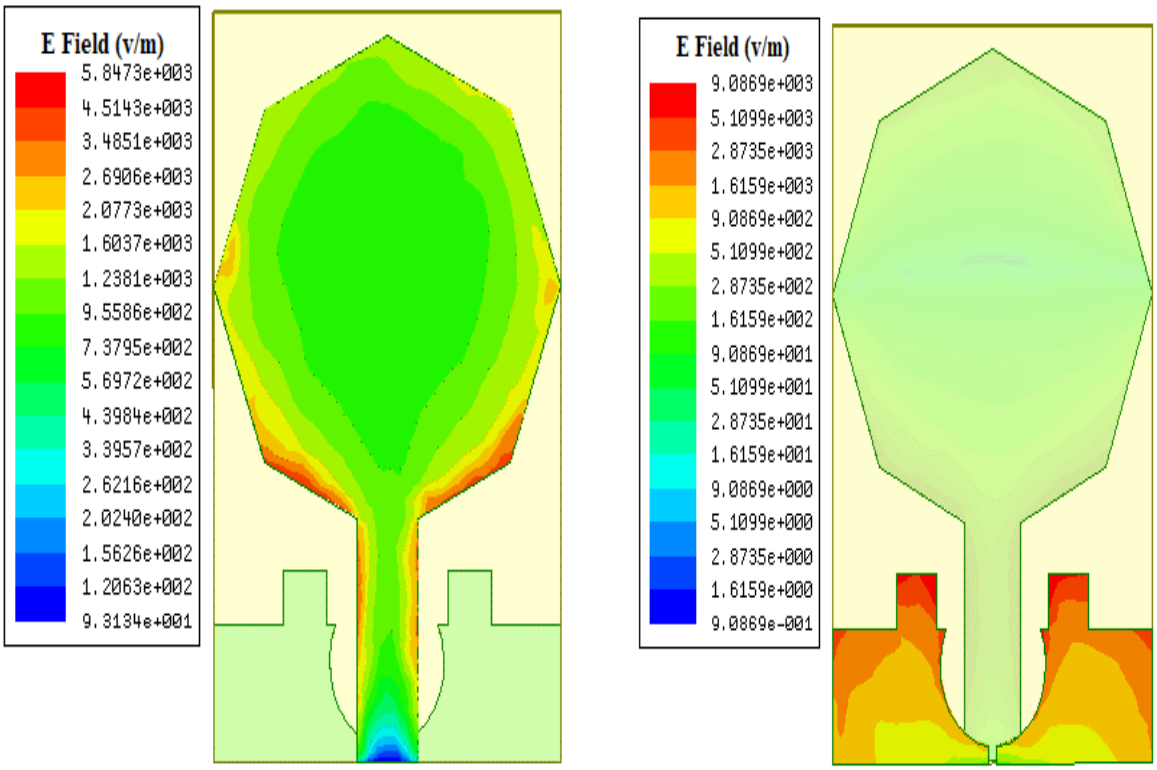

Fig. 7. Surface current distributions for monopole patch and ground planes at 2.6 GHz (color online)

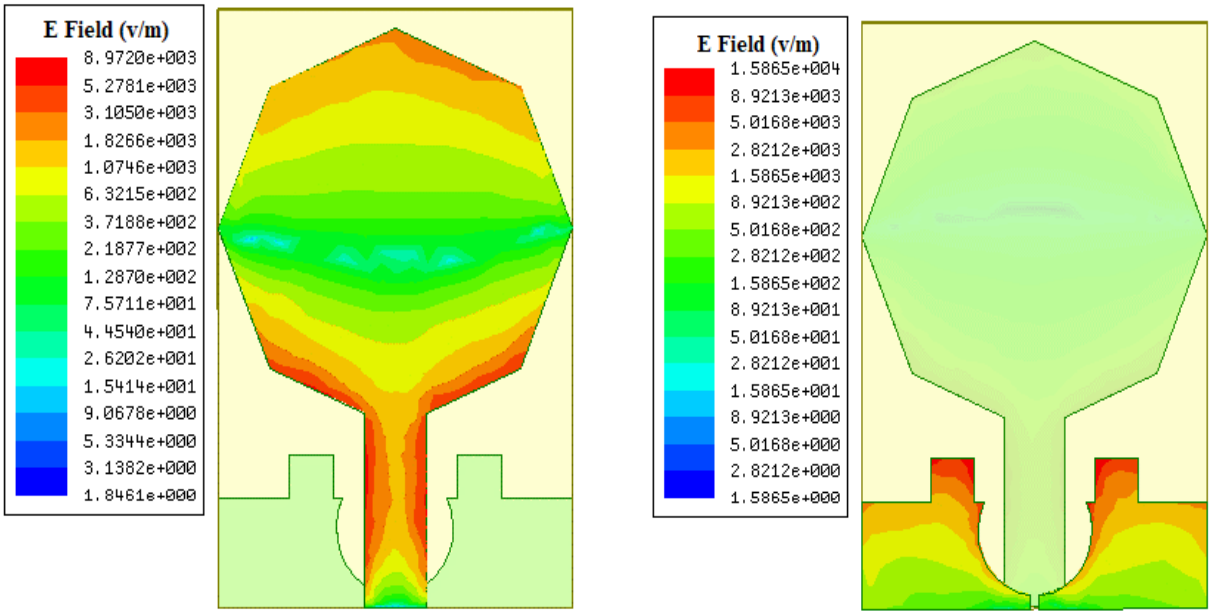

Fig. 8. Surface current distributions for monopole patch and ground planes at 5 GHz (color online)

In Table 1, the projected monopole antenna is mostly more compact and has greater impedance bandwidth than those investigated in the literature [17-22].

Table 1. Comparison of the projected monopole antenna in this article with reported ones in the literature

Ref.	**substrate/ε_r**	**Size (mm^3)**	**Dimensions in λ_o^2 @f_L**	**Bandwidth range (GHz)**
[17]	RT/duroid 5880 PTFE glass fiber / 2.2	20.5×25×3.173	0.103826	4.27- 7.58
[18]	Adhesive copper tape/ 1.75	35×30×1	0.070029	2.45 – 10.75
[19]	FR4 / 4.4	59.5×30×1.6	0.678746	5.85-6.6
[20]	LCP (Liquid Crystal Polymer) / 3	32×26.8×0.1	0.34304	6-10.8
[21]	Rogers 5880 substrate /2.2	29 × 26.5	0.082059	3.1–10.6
[22]	FR4 / 4.4	17 × 13	0.013909	2.38- 10.41 with notches at 2.68 - 3.55 and 4.5 - 5.8
Proposed	FR4 / 4.4	30×20×1.6	0.026667	2- 6

4. Fabrication and measurement

The projected antenna has been fabricated using a CNC machine, as in Fig. 9. Arinst vector network analyzer has been employed to measure the input reflection and impedance bandwidth experimentally, as shown in Fig. 10, to validate the simulated result. Differences between measurement and simulation S11 curves for the UWB antenna can be attributed to various factors. These include discrepancies in the fabrication process, differences in measurement setup and conditions, limitations of simulation models, and the impact of electromagnetic interference and environmental factors. It is common for there to be differences between measurement and simulation results for antennas, mainly in the case of UWB antennas. These differences highpoint the challenges in precisely envisaging and characterizing antenna performance, emphasizing the need for experimental validation.

Fig. 9. Snapshots of the projected monopole antenna in terms of front and back views

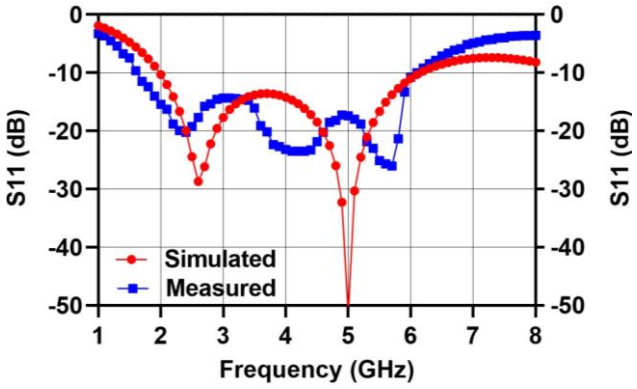

Fig. 10. Simulated and measured S11 scattering responses of the projected monopole antenna (color online)

5. Conclusions

A miniature monopole antenna for C-band/WLAN/WiMAX applications is presented in this study with UWB frequency response. From the simulation results by HFSS electromagnetic solver, it has been perceived that the C-shape on the ground plane and octagonal patch radiator are responsible for two resonance frequencies at 2.6 and 5 GHz and a wide bandwidth range from 2 to 6 GHz. The analysis shows that the dimension variations of the C-shape on the ground plane affect the antenna's performance noticeably. The omnidirectional and bi-directional far-field radiation patterns have been obtained in E-plane and H-plane, respectively. The proposed antenna is advantageous in wireless baseband transmission at a high data rate and a near-field region. The antenna has a volume of only 30 × 20 × 1.6 mm^3. Therefore, it can be easily integrated into many wireless as in medical terminals.

Acknowledgment

The researchers acknowledge the University of Mosul, University of Information Technology and Communications and Al-Farahidi University in Iraq for their support in conducting this research.

References

[1] S. Shandal, Y. Mezaal, M. Kadim, M. Mosleh, Advanced Electromagnetics **7**(4), 85 (2018).
[2] S. Shandal, Y. Mezaal, M. Kadim, Advanced Electromagnetics **7**(5), 7 (2018).
[3] O. M. Haraz, A. Sebak, K. Jamil, IEEE International Conference on Ultra-Wideband, 426 (2012).
[4] R. Mahbubu, J. Ashik, Abu Layek, A. Kumar, M. Zulfiker, Jagannath University Journal of Science **7**(II), 22 (2021).
[5] E. Hamad, M. Hamdalla, Advanced Electromagnetics **7**(3), 82 (2018).
[6] F. Mouhouche, A. Azrar, M. Dehmas, K. Djafer, Advanced Electromagnetics **7**(3), 69 (2018).
[7] L. Prasad, B. Ramesh, K. S. R. Kumar, K. P. Vinay, Advanced Electromagnetics **7**(3), 104 (2018).
[8] T. Ali, M. Saadh, R. C. Biradar, Advanced Electromagnetics **7**(4), 78 (2018).
[9] M. A. Othman, M. T. Abuelfadl, A. M. Safwat, IEEE Transactions on Antennas and Propagation 61(3) 1430 (2013).
[10] F. Abayaje, P. Febvre, International Workshop on Antenna Technology 296 (2017).
[11] F. Abayaje, S. A. Hashem, H. S. Obaid, Y. S. Mezaal, S. K. Khaleel, Periodicals of Engineering and Natural Sciences 8(1) 256 (2020).
[12] D. Kumar, T. Singh, R. Dwivedi1, S. Verma, Fourth International Conference on Computational Intelligence and Communication Networks 57 (2012).
[13] F. Abayaje, Y. S. Mezaal, B. M. Alameri, Proceedings of the Estonian Academy of Sciences **70**(2), 148 (2021).
[14] F. Abayaje, P. Febvre, AEU-International Journal of Electronics and Communication **70**(12), 1684 (2016).
[15] Q. Li, A. P. Feresidis, M. Mavridou, P. S. Hall, IEEE Transactions on Antennas and Propagation **63**(3), 1168 (2015).
[16] M. A. Othman, T. M. Abuelfadl, A. M. E. Safwat, IEEE Transactions on Antennas and Propagation **61**(3), 1430 (2013).
[17] H. T. Alrikabi, H. T. Hazim, International Journal of Interactive Mobile Technologies **15**(16), 145 (2021).
[18] F. T. Abed, H. T. S. Alrikabi, I. A. Ibrahim, IOP Conference Series: Materials Science and Engineering **870**(1), 012049 (2020).
[19] H. T. Alrikabi, A. H. M. Alaidi, A. S. Abdalrada, F. T. Abed, International Journal of Emerging Technologies in Learning (iJET) **14**(08), 23 (2019).
[20] T. Shanmuganantham, K. Balamanikandan, S. Raghavan, Int. J. Antennas Propag. **2008**, 1 (2008).
[21] M. Rahanandeh, A. S. N. Amin, M. Hosseinzadeh, P. Rezai, M. S. Rostami, IEEE Antennas and Wireless Propagation Letters **11**, 857 (2012).
[22] A. Modirkhazeni, P. Rezaei, I. A. Lafmajani, Progress in Electromagnetics Research Letters **56**, 107 (2015).

*Corresponding author: yakeen_sbah@yahoo.com